ANTIMICROBIAL AGENTS AND CHEMOTHERAPY, Dec. 1997, p. 2670–2679 Vol. 41, No. 12
0066-4804/97/$04.00+0

Population Pharmacokinetic Modeling of Isoniazid, Rifampin, and Pyrazinamide

CHARLES A. PELOQUIN,[1,2,3]* GEORGE S. JARESKO,[4,5] CHAN-LOI YONG,[6]†
ANTHER C. F. KEUNG,[6] AMY E. BULPITT,[1] AND ROGER W. JELLIFFE[5,7]

Department of Medicine, National Jewish Medical and Research Center, Denver, Colorado[1]; School of Pharmacy[2] and School of Medicine,[3] University of Colorado, Denver, Colorado; School of Pharmacy,[4] Laboratory of Applied Pharmacokinetics,[5] and School of Medicine,[7] University of Southern California, Los Angeles, California; and Hoechst Marion Roussel, Kansas City, Missouri[6]

Received 5 February 1997/Returned for modification 10 July 1997/Accepted 15 September 1997

Isoniazid (INH), rifampin (RIF), and pyrazinamide (PZA) are the most important drugs for the treatment of tuberculosis (TB). The pharmacokinetics of all three drugs in the plasma of 24 healthy males were studied as part of a randomized cross-over phase I study of two dosage forms. Subjects ingested single doses of INH at 250 mg, RIF at 600 mg, and PZA at 1,500 mg. Plasma was collected for 36 h and was assayed by high-performance liquid chromatography. The data were analyzed by noncompartmental, iterative two-stage maximum a posteriori probability Bayesian (IT2B) and nonparametric expectation maximization (NPEM) population modeling methods. Fast and slow acetylators of INH had median peak concentrations in plasma (C_{max}) of 2.44 and 3.64 μg/ml, respectively, both of which occurred at 1.0 h postdose (time of maximum concentrations of drugs in plasma [T_{max}]), with median elimination half-lives ($t_{1/2}$) of 1.2 and 3.3 h, respectively (by the NPEM method). RIF produced a median C_{max} of 11.80 μg/ml, a T_{max} of 1.0 h, and a $t_{1/2}$ of 3.4 h. PZA produced a median C_{max} of 28.80 μg/ml, a T_{max} of 1.0 h, and a $t_{1/2}$ of 10.0 h. The pharmacokinetic behaviors of INH, RIF, and PZA were well described by the three methods used. These models can serve as benchmarks for comparison with models for other populations, such as patients with TB or TB with AIDS.

Isoniazid (INH), rifampin (RIF), and pyrazinamide (PZA) are the most important drugs for the treatment of disease caused by drug-susceptible *Mycobacterium tuberculosis*. The standard short-course treatment consists of treatment with all three drugs for 2 months, followed by treatment with INH and RIF given either daily or intermittently for 4 more months (1, 17). While INH and RIF are better studied, limited information exists regarding the pharmacokinetics of PZA in healthy or infected individuals, and population models have not been described for any of these drugs (6, 10, 15, 18, 23). We examined the kinetic behaviors of INH, RIF, and PZA in healthy volunteers using three techniques. These models describe concentrations in plasma and kinetic behavior under optimal conditions and can be used as benchmarks for comparison with models for samples obtained in other clinical settings.

(Part of this study was presented at the 36th Interscience Conference on Antimicrobial Agents and Chemotherapy, New Orleans, La. 15 to 18 September 1996 [20a].)

MATERIALS AND METHODS

The study was designed as a two-way, randomized, crossover study of INH, RIF, and PZA. The study compared each oral dosage form separately versus the combination product containing all three drugs (Rifater). We report here the results for the individual dosage forms.

The study protocol followed the guidelines of the Helsinki Declaration of 1975 and its amendments and was approved by the institutional review board. Written informed consent was obtained from each subject before the study. Twenty-four normal, healthy male volunteers were scheduled to participate in the study. Subjects were eligible to participate if they were between the ages of 19 and 45 years and weighed within 10% of their calculated ideal body weight (1983 Metropolitan Height and Weight Study and 1979 Build Study) (2). Individuals were excluded if they had histories of tuberculosis or of exposure to INH, RIF, or PZA, a major illness, drug or alcohol abuse, or blood donation within 30 days prior to the study. Subjects were determined to be healthy on the basis of a medical history, physical examination, and laboratory studies including serum chemistries, complete blood count with differential, urinalysis with microscopy, 12-lead electrocardiogram, and urine drug abuse screen. The subjects agreed to refrain from the use of medications and alcohol during the entire study period.

Experimental design. The subjects were housed at the study center from 12 h before to 36 h after dosing. They fasted from 10 p.m. before the doses were given until 4 h afterward. Water was allowed ad libitum until 2 h before the doses were administered. The subjects took three tablets each containing 500 mg of PZA (1,500 mg of PZA; lot no. 342-177; Lederle Laboratories) along with 2.5 tablets each containing 100 mg of INH (250 mg of INH; lot no. 2F065; Eon Laboratories) and 2 capsules each containing 300 mg of RIF (600 mg of RIF; lot no. 645CB; Hoechst Marion Roussel). The subjects were allowed to ingest water ad libitum after the doses were given, and identical, nutritionally balanced meals were provided to all subjects during the remainder of the study period. There was a 14- to 21-day washout period between each study period.

Sample collection. Each blood sample (18 ml) was collected by venipuncture and was placed into prechilled vacuum tubes containing sodium heparin. The blood samples were collected predosing and at 0.5, 1, 1.5, 2, 2.5, 3, 4, 6, 9, 12, 18, 24, 30, and 36 h after the doses were given. Blood samples for INH and PZA concentration determinations were centrifuged, and the plasma was harvested into labeled plastic tubes. Blood samples for RIF concentration determination were centrifuged, and 3 ml of the plasma was harvested into labeled plastic tubes containing 30 μl of L-ascorbic acid (20 mg/ml), which served as an antioxidant. The plasma samples were frozen at −70°C within 40 min of collection and remained frozen until analysis.

Sample analysis, INH. All high-performance liquid chromatography (HPLC) procedures for analysis of samples for the INH concentration were performed with the following equipment: a Waters (Milford, Mass.) model 510 pump, a Waters model 710 fixed-volume autosampler with cooler, and a Waters model 486 UV detector. The standard curves for the INH concentration in plasma covered a range of from 0.1 to 12 μg/ml. The absolute recovery of INH from plasma was 50.2%. The within-batch precision (percent coefficient of variation [CV]) of validation quality control samples was 1.3 to 8.8%, and the batch-to-batch precision was 3.4 to 11.0%. The batch-to-batch assay error pattern was determined by six injections each of spiked plasma samples containing 0.10, 0.20, 0.60, 1.80, 5.99, 8.98, 10.71, and 12.04 μg of INH per ml over 3 days of validation (11). The means, standard deviations, and CVs were determined at each concentration. The overall assay error pattern was determined by fitting a third-order polynomial to the plot of the assay standard deviations (Y) versus the means (X), producing a formula $y = 0.01000 + 0.17993(x) + 0.026542(x^2) + 0.0011821(x^3)$ ($R^2 = 0.894$) (11). This polynomial describing the assay error

* Corresponding author. Mailing address: Infectious Disease Pharmacokinetics Laboratory, National Jewish Medical and Research Center, 1400 Jackson St., Denver, CO 80206.

† Present address: Boehringer Ingelheim Pharmaceuticals, Inc., Ridgefield, CT 06877.

pattern was included in the plasma INH concentration data analysis by using the NPEM2 software described below. A simplified first-order polynomial error pattern, $y = 0.01000 + 0.17993(x)$, was also used for comparison (data not shown).

Sample analysis, RIF. All HPLC procedures for analysis of the samples for the RIF concentration were performed with the following equipment: a Spectra Physics (San Jose, Calif.) model P-4000 pump, a Spectra Physics model AS 3000 fixed-volume autosampler, and a Spectra Physics model UV 150 UV detector. The standard curves for the RIF concentration in plasma covered a range of from 0.4 to 50 μg/ml. The absolute recovery of RIF from plasma was 89.5%. The within-batch precision (percent CV) of validation quality control samples was 1.0 to 7.5%, and the batch-to-batch precision was 1.5 to 6.6%. The batch-to-batch assay error pattern was determined by six injections each of spiked plasma samples containing 0.40, 0.86, 2.57, 7.51, 24.98, 37.46, 44.99, and 50.04 μg of RIF per ml over 3 days of validation (11). The means, standard deviations, and CVs were determined at each concentration. The overall assay error pattern was determined by fitting a second-order polynomial to the plot of the assay standard deviations (Y) versus the means (X), producing a formula $y = 0.09900 - 0.00870(x) + 0.01000(x^2)$ ($R^2 = 0.784$) (11). This polynomial describing the assay error pattern was included in the plasma RIF concentration data analysis by using the NPEM2 software described below. A simplified first-order polynomial error pattern, $y = 0.09900 + 0.07(x)$, was also used for comparison (data not shown).

Sample analysis, PZA. All HPLC procedures for analysis of the samples for the PZA concentration were performed with the following equipment: a Waters model 600 pump and model 600E controller, a Gilson (Middleton, Wis.) model 231 fixed-volume autosampler, and a Spectra Physics model UV 2000 UV detector. The standard curves for the PZA concentration in plasma covered a range of from 2 to 50 μg/ml. The absolute recovery of PZA from plasma was 106.6%. The within-batch precision (percent CV) of validation quality control samples was 1.2 to 9.6%, and the batch-to-batch precision was 1.8 to 8.9%. The batch-to-batch assay error pattern was determined by six injections each of spiked plasma samples containing 2, 4, 10, 25, 40, and 50 μg of PZA per ml over 3 days of validation (11). The means, standard deviations, and CVs were determined at each concentration. The overall assay error pattern was determined by fitting a third-order polynomial to the plot of the assay standard deviations (Y) versus the means (X), producing a formula $y = 0.049067 + 0.030526(x) - 0.0014081(x^2) + 0.00005(x^3)$ ($R^2 = 0.988$) (11). This polynomial describing the assay error pattern was included in the plasma PZA concentration data analysis by using the NPEM2 software described below. A simplified first-order polynomial error pattern, $y = 0.049067 + 0.030526(x)$, was also used for comparison (data not shown).

Pharmacokinetic analysis. Each drug was analyzed separately by the three methods described below.

For the noncompartmental analysis (NCA), concentrations in plasma below the quantification lower limit (BQL) were recorded as BQLs and were treated as zeros in averaging the concentrations at a given collection time. The observed maximal concentration in plasma (C_{max}) and the time at which C_{max} occurred (T_{max}) were determined for each subject by inspection of the plasma concentration-versus-time graphs. The apparent elimination rate constant (K) was determined as the slope of the terminal portion of the natural log concentration-versus-time plot by unweighted linear regression analysis. The half-life ($t_{1/2}$) in plasma was calculated as $\ln(2)/K$. The area under the plasma concentration-versus-time curve from time zero to the last quantifiable concentration (AUC_{0-C^*}) was determined by the linear trapezoidal rule. The area under the plasma concentration-versus-time curve from time zero to infinity ($AUC_{0-\infty}$) was determined as $AUC_{0-C^*} + C^*/K$. The apparent total body clearance (CL) was calculated as dose (F)/$AUC_{0-\infty}$, where F is the fraction of the dose absorbed (7). An estimate of the volume of distribution (V) was calculated by the area method [dose (F)/(K) $AUC_{0-\infty}$] (7). V was expressed as liters per kilogram of actual body weight. The potential for accumulation of these drugs with multiple doses was evaluated by using the principle of superposition (7). The accumulation of PZA with eight daily doses was simulated by using the data for the median concentration in plasma from 0 to 24 h and was extrapolated from 24 h to day 8 by using the median value of K.

Population pharmacokinetic models were made by using NPEM2, USC*PACK, version 10.6, software (12). F was arbitrarily fixed at 1. A one-compartment open model with first order absorption and elimination was used. The absorption and elimination $t_{1/2}$s were calculated as $\ln(2)/k_a$ (where k_a is the absorption rate constant) and $\ln(2)/K$, respectively. The first part of NPEM2, the iterative two-stage maximum a posteriori probability Bayesian population modeling portion (IT2B), generated each subject's IT2B parameter estimates and calculated the probable range of these values to be reanalyzed by the nonparametric approach (12). The second part, the nonparametric expectation maximization algorithm (NPEM) portion, then provided the joint probability density functions of the final pharmacokinetic parameters (12). For each drug, three parameters were fit simultaneously in two sequential analyses (k_a, V, and K, followed by k_a, V, and CL). This was done in order to verify the results and to address problems that may arise with one set of parameters but not the other, such as the "flip-flop" problem of structural identifiability. The log-likelihood criterion was used to determine the best fit among candidate models. In addition, Bayesian posterior parameter joint densities for individual subjects were estimated starting from the population parameter joint density and continuing to an analysis of the data for each subject to obtain the individual parameter joint densities.

Parameter estimates were compared on a subject-by-subject basis with the results of NCA by using JMP statistical software (see below). Each subject's IT2B parameter estimates were observed. In addition, the NPEM program produced similar individual estimates by analyzing the data for each subject, as described above. The NPEM population parameter means and medians and their likelihoods also were compared to the population mean and median parameter estimates obtained by the two previous methods. Creatinine clearance (CL_{CR}) was calculated by the method of Cockroft and Gault (4).

D-optimal sampling time analysis was performed by using ADAPT II software and the NPEM parameter estimates (5). Because this software does not accommodate third-order polynomial error patterns, only the first-order error patterns described above were used. Sampling times were analyzed by using the parameters k_a, V, and K over the period from 0.5 to 24.0 h, with various initial sampling times. A two-sample strategy (achieved by fixing k_a and fitting only V and K) and a three-sample strategy (achieved by fitting all three parameters) were tested. In addition, an analysis of C_{max} was performed for each drug over the period from 0.5 to 3.0 h, calculating the maximum, median, and minimum percentage of the measured concentration divided by C_{max}.

Statistical analysis. Data analysis was performed by using JMP software (version 3.1.6; SAS Institute, Cary, N.C.), with supplemental analyses done with Excel software (version 4.0; Microsoft, Seattle, Wash.), and USC*PACK software, version 10.6. Frequency distributions (obtained by using JMP software) included plots of the data, distribution curves to test for normality, parametric and nonparametric measures of central tendency and dispersion, and the Shapiro-Wilk W test for normality. Means ± standard deviations (SDs) are reported. The percent CV was calculated as (SD/mean) multiplied by 100%. Correlation analysis (performed with JMP software) was performed across the subject and outcome variables by parametric and nonparametric techniques. The dependence of outcome variables (the pharmacokinetic parameters) upon subject characteristics (demographic data such as age, weight, CL_{CR}, etc.) was determined by using Y-by-X analyses, one parameter at a time (by using JMP software). Subsequently, models with multiple X variables were constructed by using forward addition and backward deletion. Differences between groups (by using JMP software) were determined by using the analysis of log likelihood with the Pearson chi-square statistic (contingency tables), Student's t test or analysis of variance (two or more than two groups, respectively) of normally distributed data (one-way layouts and linear regression), the Wilcoxon or the Kruskal-Wallis tests (rank sums) for nonnormally distributed data (one-way layouts), and the Whole-Model test table with chi-square statistic (by logistic regression). Differences between groups or correlations between parameters and covariates were considered statistically significant at a P value of ≤ 0.05.

RESULTS

Twenty-four male subjects (23 Caucasians and 1 Hispanic) completed the study. The mean age was 27.5 ± 7.1 years (range, 19 to 45 years), and the mean weight was 76.9 ± 11.0 kg (range, 60.0 to 101.4 kg). These demographic values were similar for fast versus slow INH acetylators and for the 4 smokers versus the 20 nonsmokers. All subjects were within 10% of their estimated lean body weight. The subjects received 250 mg of INH (3.3 ± 0.5 mg/kg of body weight), 600 mg of RIF (8.0 ± 1.1 mg/kg), and 1,500 mg of PZA (19.9 ± 2.8 mg/kg). All subjects denied the use of any nonprotocol medications during the study period. CL_{CR} estimates ranged from 72 to 130 ml/min.

Absorption: INH. The absorption characteristics of INH obtained by NCA are described in Table 1, and the mean plasma INH concentration-versus-time profile across the 24 subjects is presented in Fig. 1. Twenty of the 24 subjects had T_{max} values of ≤1.0 h, while 23 of the 24 subjects had T_{max} values of ≤2.0 h. The C_{max} and $AUC_{0-\infty}$ values were higher in slow acetylators ($P = 0.0008$ and <0.0001, respectively; t test). In addition, the INH concentrations at 4 and 6 h, often cited as discriminating tests for acetylator status, were higher in slow acetylators ($P < 0.0001$ each; t test) (21). T_{max} values were similar for fast and slow acetylators. Variability in the absorption of INH was found to be moderate (Table 1). The CVs for the C_{max} and $AUC_{0-\infty}$ values were narrow, regardless of acetylator status, while T_{max} values were more variable for slow acetylators than for fast acetylators. Because the usual clinical dose of INH is 300 mg, Table 1 includes extrapolated values for this dose

TABLE 1. Absorption characteristics of INH following the administration of a 250-mg dose calculated by noncompartmental methods and extrapolated to the standard 300-mg dose

Dose and group	C_{max} (μg/ml)				T_{max} (h)				$AUC_{0-\infty}$			
	Mean ± SD	Median	Range	% CV	Mean ± SD	Median	Range	% CV	Mean ± SD	Median	Range	% CV
250 mg												
Actual, all subjects	3.14 ± 0.92	2.98	1.04–5.11	29.4	1.06 ± 0.58	1.00	0.50–3.00	54.3	13.82 ± 6.87	14.74	2.96–26.39	49.7
Actual, fast acetylators (n = 8)	2.33 ± 0.59	2.44	1.04–2.96	25.3	0.88 ± 0.23[a]	1.00	0.50–1.00	26.1	5.51 ± 1.16	5.86	2.96–6.95	21.0
Actual, slow acetylators (n = 16)	3.55 ± 0.78	3.64	2.17–5.11	22.0	1.16 ± 0.68[a]	1.00	0.50–3.00	58.6	17.98 ± 4.05	17.31	13.10–26.39	22.5
300 mg[b]	3.77 ± 1.11	3.58	1.25–6.13		1.06 ± 0.58[a]	1.00	0.50–3.00		16.59 ± 8.24	17.68	3.55–31.67	

[a] Interpolated.
[b] Extrapolated, all subjects.

across all subjects. The extrapolated median C_{max} values for fast and slow acetylators after the administration of 300 mg of INH are 2.93 and 4.37 μg/ml, respectively. Simulations for eight multiple daily doses of INH showed no significant INH accumulation.

Parameter estimates, INH. Table 2 shows the parameter estimates for INH following administration of the 250-mg dose, as calculated by the three methods across all subjects. The NPEM model estimates for k_a and absorption $t_{1/2}$ showed considerable variability, although the median estimates were fairly close to those found with the IT2B model. The determination of k_a was not pursued by NCA. The three models (the NCA, IT2B, and NPEM models) all produced similar estimates for V, CL, K, and $t_{1/2}$, with the IT2B and NPEM models producing very similar estimates. NCA produced somewhat larger estimates for V and $t_{1/2}$. All three models also revealed two subgroups of INH metabolizers on the basis of differences in CL, K, and $t_{1/2}$. These subjects were easily identified on the basis of the elimination $t_{1/2}$: the 8 fast acetylators all had $t_{1/2}$s of $<$2 h, while the 16 slow acetylators all had $t_{1/2}$s of $\geq$2 h (Fig. 2) (15, 18). Much of the variability found in the CL, K, and $t_{1/2}$ estimates in Table 2 was due to the inclusion of data for both acetylator groups in the analysis. Data for fast and slow acetylators were subsequently analyzed separately (Table 3).

Fast acetylators had significantly larger CL and K values and significantly lower $t_{1/2}$ values compared to those for slow acetylators, regardless of the method used ($P < 0.0001$ for all three comparisons; t test). Fast acetylators also had significantly larger estimates for V compared to those for slow acetylators ($P < 0.0016$; t test). The differences in k_a did not reach statistical significance ($P = 0.6054$). Analysis of the individual subject densities with the NPEM model did not reveal any modeling problems, such as the flip-flop problem of structural identifiability.

The median parameter estimates obtained by using the first-order polynomial error pattern were within ±8% of those derived by using the third-order polynomial, although the associated ranges for V were somewhat wider with the first-order error pattern.

D-optimal sampling times, INH. The D-optimal sampling times for all subjects over the period from 0.5 to 24.0 h were 0.5 and 16.6 h for the two-sample strategy and 0.5, 2.9, and 17.2 h for the three-sample strategy. The data in Table 4 indicate that the C_{max} for the 1.0-h sample came closest to the C_{max}s for the greatest number of the 24 subjects. The D-optimal sampling times for fast acetylators over the period from 0.5 to 24.0 h were 0.5 and 7.0 h for the two-sample strategy and 0.5, 2.6, and 7.6 h for the three-sample strategy. The data in Table 4 indicate that the 1.0-h sample concentrations were closest to the C_{max}s for the greatest number of the eight subjects. The D-optimal sampling times for slow acetylators over the period from 0.5 to 24.0 h were 0.5 and 18.7 h for the two-sample strategy and 0.5, 2.0, and 19.1 h for the three-sample strategy. The data in Table 4 indicate that the 1.0-h sample concentrations were closest to the C_{max} for the greatest number of the 16 subjects.

Covariate analysis, INH. Because the three methods produced similar estimates for the pharmacokinetic parameters (excluding k_a), the results obtained by the IT2B method were chosen as being representative for further analysis with the JMP statistical software. This analysis was performed to determine correlations between the individual IT2B parameter estimates and the individual subject characteristics or covariates. Because some of the items tested were not normally distributed, the nonparametric measures of association are reported here. As expected, there was a positive correlation between height and weight ($r = 0.5125$; Spearman $P = 0.0104$).

The pharmacokinetic indices and parameter estimates were not correlated strongly with age. CL, K, and $t_{1/2}$ correlated with C_{max} ($r = 0.8609$ and $P < 0.0001$ for CL; $r = \pm 0.6991$ and $P = 0.0013$ for K and $t_{1/2}$), given the higher C_{max} in slow acetylators (described above). V (in liters per kilogram) also correlated with C_{max}. The CL, K, and $t_{1/2}$ of INH did not correlate with CL_{CR} ($r = 0.1070$ and ± 0.2530 for CL and for K and $t_{1/2}$, respectively). The pharmacokinetic parameters for the 4 smokers were not significantly different from those for the 20 nonsmokers. $t_{1/2}$s calculated by using only concentrations in serum at 2 and 6 h, an alternative method of assessing acetylator

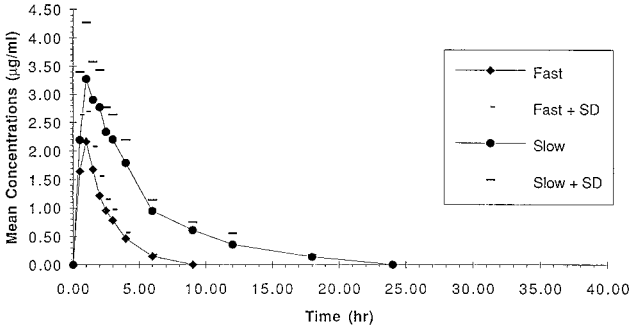

FIG. 1. Mean plasma INH concentrations across the 24 subjects following administration of a 250-mg dose of INH.

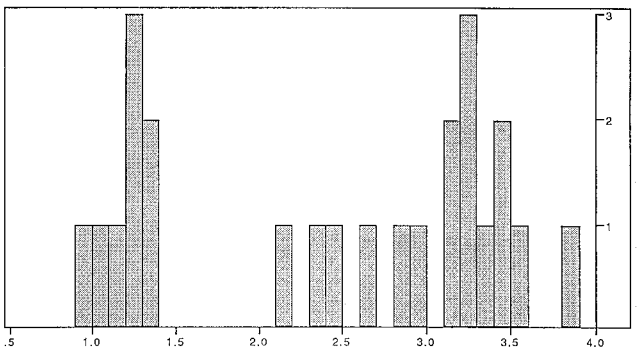

FIG. 2. Frequency histogram of INH $t_{1/2}$ from IT2B model for fast and slow acetylators combined. The *y* axis shows the number of subjects; the *x* axis shows $t_{1/2}$. These data reveal only one population of fast acetylators, all of whom had $t_{1/2}$s of less than 2 h.

status, were highly correlated with $t_{1/2}$ obtained by using NCA ($r = 0.7885$; $P < 0.0001$).

Absorption, RIF. The absorption characteristics for RIF obtained by NCA are described in Table 5, and the mean plasma RIF concentration-versus-time profile across the 24 subjects is presented in Fig. 3. For 22 of 24 subjects T_{max} values were ≤2.0 h. Variability in the C_{max}, $AUC_{0-\infty}$, and T_{max} values was modest across the 24 subjects, although the C_{max} values covered a 2.6-fold range. Simulations for eight multiple daily doses of RIF showed no significant accumulation.

Parameter estimates, RIF. Table 6 presents the parameter estimates for RIF following administration of the 600-mg dose as calculated by the three methods. The determination of k_a by NCA was not pursued.

The serum RIF concentration data and NPEM models revealed two groups of RIF absorbers: smooth absorbers and those who had early low concentrations followed by rapid absorption (low absorbers; Table 6). Most smooth absorbers (11 of 14) had no measurable concentration at 0.5 h postdosing. In contrast, 8 of 10 low absorbers had concentrations of RIF of <2.5 μg/ml at 0.5 h postdosing and much larger concentrations (>9 μg/ml) at 1.0 h. Review of the first and second measurable concentrations in plasma (*C1* and *C2*, respectively) revealed that smooth absorbers had *C2*/*C1* ratios of <4.0, with a median ratio of 1.46 and a range of 1.01 to 3.27. Low absorbers had *C2*/*C1* ratios of >4.0, with a median ratio of 8.59 and a range of 4.14 to 15.20. *C2*/*C1* ratios were negatively correlated with the individual (population of 1) NPEM model k_a estimates (Spearman rho = −0.7470; $P < 0.0001$). T_{max} was not significantly later in low absorbers ($P = 0.4924$; Wilcoxon). Simulations for eight multiple daily doses of RIF showed no significant accumulation.

Several additional models were created for smooth and low absorbers separately, with and without absorption lag phases. The lag phase was created by arbitrarily altering the time of dose in the PASTRX data files in the USC*PACK software to 0.25 h prior to *C1*. For 8 of 10 low absorbers, the lag time was 15 min; for the remaining 2 low absorbers the lag time was 45 min. The initial models (no lag) showed large differences in the calculated k_a between smooth and low absorbers, leading to large variances in the population estimates for k_a (all subjects, no lag phase; Table 7). On the basis of comparisons of log likelihood, the use of a lag phase moderately improved the models for the smooth absorbers, while it improved the models for the low absorbers still more. In each case, the k_a increased and the absorption $t_{1/2}$ decreased with the inclusion of the lag phase. In contrast, estimates of *V*, CL, *K*, and $t_{1/2}$ were similar

TABLE 2. Values of pharmacokinetic parameters obtained by various methods for all subjects following administration of an INH dose of 250 mg

Method	k_a (h^{-1})			Absolute $t_{1/2}$ (h)			*V* (liters/kg)			CL (liters/h)			*K* (h^{-1})			$t_{1/2}$ (h)		
	Mean ± SD	Median	Range	Mean ± SD	Median	Range	Mean ± SD	Median	Range	Mean ± SD	Median	Range	Mean ± SD	Median	Range	Mean ± SD	Median	Range
NCA	NC[a]	NC	NC	NC	NC	1.04 ± 0.23	0.98	0.78–1.77	25.72 ± 18.39	16.98	9.47–84.46	0.31 ± 0.16	0.21	0.16–0.63	2.80 ± 1.11	3.23	1.10–4.43
IT2B	2.57 ± 1.59	2.49	0.34–5.08	0.51 ± 0.51	0.29	0.14–2.03	0.95 ± 0.16	0.88	0.77–1.37	26.63 ± 17.88	17.01	9.54–73.75	0.35 ± 0.18	0.25	0.18–0.70	2.45 ± 0.98	2.74	0.99–3.85
NPEM	6.55 ± 8.05	2.10	0.39–28.53[b]	0.11[c]	0.33	0.02–1.79[b]	0.97 ± 0.21	0.89	0.73–1.49[b]	26.76 ± 18.33	16.81	9.28–77.25[b]	0.35 ± 0.19	0.24	0.18–0.75[b]	2.00[c]	2.89	0.92–3.95[b]

[a] NC, not calculated.
[b] Approximate range, from 2.5 to 97.5%, as calculated by NPEM.
[c] Calculated as $\ln(2)/k_a$ or $\ln(2)/K$ from the population means and not across the individual point estimates. Therefore, no SD is included.

TABLE 3. Values of pharmacokinetic parameters obtained by various methods for fast and slow INH acetylators following administration of an INH dose of 250 mg

Method, acetylator speed	k_a (h^{-1})			Absolute $t_{1/2}$			V (liters/kg)			CL (liters/h)			K (h^{-1})			$t_{1/2}$ (h)		
	Mean ± SD	Median	Range	Mean ± SD	Median	Range	Mean ± SD	Median	Range	Mean ± SD	Median	Range	Mean ± SD	Median	Range	Mean ± SD	Median	Range
NCA, fast (n = 8)	NC[a]	NC	NC	NC	NC	NC	1.23 ± 0.27	1.10	0.98–1.77	48.15 ± 15.19	42.70	35.97–84.46	0.52 ± 0.07	0.53	0.39–0.63	1.35 ± 0.20	1.30	1.10–1.78
IT2B, fast (n = 8)	2.17 ± 1.13	1.94	0.53–3.93	0.46 ± 0.37	0.36	0.18–1.31	1.16 ± 0.12	1.12	1.02–1.41	49.96 ± 10.97	46.74	37.36–72.14	0.61 ± 0.03	0.60	0.57–0.65	1.14 ± 0.05	1.15	1.07–1.22
NPEM, fast (n = 8)	4.2 ± 5.64	2.00	0.52–19.69	0.17[c]	0.35	0.04–1.32[b]	1.10 ± 0.31	1.15	0.37–1.49[b]	49.96 ± 12.48	44.40	37.44–77.85[b]	0.59 ± 0.07	0.58	0.48–0.76[b]	1.17[c]	1.20	0.92–1.43[b]
NCA, slow (n = 16)	NC	NC	NC	NC	NC	NC	0.94 ± 0.13	0.90	0.78–1.25	14.51 ± 2.92	14.44	9.47–19.08	0.20 ± 0.02	0.20	0.16–0.25	3.53 ± 0.41	3.54	2.81–4.43
IT2B, slow (n = 16)	2.72 ± 1.70	3.23	0.38–4.88	0.51 ± 0.51	0.22	0.14–1.83	0.87 ± 0.08	0.86	0.77–1.06	15.09 ± 3.02	15.19	9.64–21.17	0.22 ± 0.03	0.22	0.19–0.27	3.13 ± 0.35	3.18	2.53–3.73
NPEM, slow (n = 16)	6.69 ± 7.47	3.54	0.30–20.86[b]	0.10[c]	0.20	0.03–2.31[b]	0.89 ± 0.11	0.87	0.73–1.18[b]	14.96 ± 3.29	15.17	9.12–22.88[b]	0.22 ± 0.04	0.21	0.17–0.31[b]	3.15[c]	3.26	2.22–4.07[b]

[a] NC, not calculated.
[b] Approximate range, from 2.5 to 97.5%, as calculated by NPEM.
[c] Calculated as $\ln(2)/k_a$ or $\ln(2)/K$ from the population means and not across the individual point estimates. Therefore, no SD is included.

for all models except the low absorbers with no lag phase. Combining the smooth and low absorber subgroups and using the lag phase produced an alternative model. In this model, 11 of 14 smooth absorbers required a lag phase of 45 min; the remaining 3 subjects required a lag phase of 15 min. Based on log likelihood, a slightly better model was produced by using the lag phase for all subjects. The latter model estimated a faster k_a and a shorter absorption $t_{1/2}$.

The five models (NCA, the IT2B model with or without a lag phase, and the NPEM model with or without a lag phase) all produced very similar estimates of V, with NCA producing the smallest estimate. The no-lag-phase IT2B and NPEM models produced the largest estimates of CL. The estimates for K covered a narrow range, with NCA producing the largest estimate and the NPEM model with a lag phase producing the smallest estimate (Table 7). Analysis of individual subject densities by the NPEM model did not reveal any modeling problems, such as the flip-flop problem of structural identifiability.

The median parameter estimates obtained by using the first-order polynomial error pattern were within ±9% of those derived by using the third-order polynomial except for V, which was 18% lower by using the first-order error pattern. The associated ranges were somewhat narrower with the first-order error pattern.

D-optimal sampling times, RIF. The D-optimal sampling times (no lag phase) for all subjects over the period from 0.5 to 24.0 h were 1.2 and 14.3 h for the two-sample strategy and 0.6, 7.1, and 17.2 h for the three-sample strategy. The D-optimal sampling times (with lag phase) for all subjects over the period from 0.5 to 24.0 h were 0.7 and 12.2 h for the two-sample strategy and 0.5, 2.9, and 14.6 h for the three-sample strategy. The data in Table 4 indicate that the 1.5-h sample concentrations were closest to the C_{max}s for the greatest number of the 24 subjects.

Covariate analysis, RIF. As described for INH, the results for RIF obtained by the IT2B method were analyzed with JMP software, and the nonparametric measures of association are reported. The pharmacokinetic indices and parameter estimates were not correlated strongly with age. The taller and heavier subjects had lower C_{max} values ($r = -0.6107$ and $P = 0.0015$ and $r = -0.6348$ and $P = 0.0009$, respectively). The taller and heavier subjects also had lower $AUC_{0-\infty}$ values ($r = -0.6739$ and $P = 0.0003$ and $r = -0.4397$ and $P = 0.0317$, respectively). CL (in liters per hour) was largest in the tallest and heaviest subjects ($r = -0.6739$ and $P = 0.0003$ and $r = -0.4394$ and $P = 0.0317$, respectively). K and $t_{1/2}$ were not correlated strongly with CL_{CR} ($r = \pm 0.1509$ and $P = 0.4815$ for K and $t_{1/2}$). RIF CL did correlate weakly with CL_{CR} ($r = 0.4078$; $P = 0.0479$). In addition, there was a negative correlation between both C_{max} and $AUC_{0-\infty}$ and CL_{CR}, which was expected given their correlations with CL. The pharmacokinetic parameters for the 4 smokers were not significantly different from those for the 20 nonsmokers.

Absorption, PZA. The absorption characteristics for PZA obtained by NCA are described in Table 8, and the mean plasma PZA concentration-versus-time profile across the 24 subjects is presented in Fig. 4. All subjects had T_{max} values of ≤2.0 h. Variability in the absorption of PZA was found to be fairly small.

Simulated multiple daily doses of PZA obtained by using the median NPEM K value showed that on day 4, after six to seven PZA $t_{1/2}$s, the 1-h PZA concentration (C_{max}) was 24.6% higher than that on day 1 but only 3.8% higher than that on day 2 and 0.6% higher than that on day 3. Subsequent simulated C_{max} values remained constant. Given the day 1 C_{max} range of 21.70

TABLE 4. Concentrations collected from 0.5 to 3 h expressed as a percentage of C_{max}

Time postdose (h)	Percent														
	INH, all			INH, fast acetylators			INH, slow acetylators			RIF			PZA		
	High	Median	Low	High	Median	Low	High	Median	Low	High	Median	Low	High	Median	Low
0.5	100.00	67.75	9.20	100.00	67.75	12.45	100.00	67.36	9.20	43.45	12.32	4.92	100.00	67.70	20.76
1.0	100.00	100.00	52.19	100.00	100.00	61.82	100.00	99.59	52.19	100.00	88.36	8.45	100.00	100.00	62.63
1.5	100.00	81.35	58.47	96.15	72.94	58.47	100.00	82.02	59.16	100.00	97.06	66.81	100.00	94.86	66.32
2.0	100.00	70.65	32.09	78.85	55.89	32.10	100.00	76.46	61.54	100.00	89.20	62.17	100.00	91.33	62.69
2.5	90.32	56.73	30.07	56.73	38.77	30.07	90.32	70.59	46.25	100.00	83.34	56.80	96.95	87.62	58.40
3.0	100.00	56.39	27.02	44.18	33.17	27.02	100.00	67.00	36.34	100.00	63.50	46.29	94.14	83.59	56.78

[a] High, median, and low indicate the range of percentages of C_{max} determined at each time point.

to 42.64 μg/ml (Table 7), the calculated steady-state range for PZA (dose of ~20 mg/kg was 27.03 to 53.12 μg/ml.

Parameter estimates, PZA. Table 9 presents the parameter estimates for PZA following administration of the 1,500-mg dose calculated by the three methods. The determination of k_a was not pursued by NCA. All methods produced similar estimates and ranges for V, CL, K, and $t_{1/2}$. The IT2B and NPEM methods also produced similar median estimates of k_a and the absorption $t_{1/2}$. However, the NPEM method produced a wider range of k_a estimates, resulting in an increase in the mean and standard deviation for k_a compared to those obtained by the IT2B approach.

Analysis of the individual subject joint densities from the NPEM portion of the USC*PACK software revealed the potential for encountering the flip-flop problem of structural identifiability known to be present with the pharmacokinetic model used. This was seen when the K, k_a, and V parameterization was used but not when CL, k_a, and V were used. One of the 24 subjects had a reversal of the K and k_a values relative to the values for the other 23 subjects, along with a reduction in the apparent V by an order of magnitude. Elimination of that subject's data file from the sample resulted in values for another 1 of the remaining 23 subjects being flip-flopped in the subsequent model, and so on with smaller samples. This problem was eliminated by serial adjustment of the initial ranges for K, k_a, and V used by the NPEM analysis. By gradually widening the initial range for k_a while narrowing those for K and V, models without the flip-flop were obtained.

The median parameter estimates obtained by using the first-order polynomial error pattern were within ±2% of those derived by using the third-order polynomial, and the associated ranges were very similar with both error patterns.

D-optimal sampling times, PZA. The D-optimal sampling times for all subjects over the period from 0.5 to 24.0 h were 0.6 and 24.0 h for the two-sample strategy and 0.5, 2.6, and 24.0 h for the three-sample strategy. The data in Table 4 indicate that the 1.0-h sample concentrations were closest to C_{max}s for the greatest number of the 24 subjects.

Covariate analysis, PZA. As described for INH, the results for PZA obtained by the IT2B method were analyzed with JMP software, and the nonparametric measures of association are reported. There was a trend for the taller and heavier subjects to have lower C_{max} values ($r = -0.4949$ and $P = 0.0140$ and $r = -0.5695$ and $P = 0.0037$, respectively). C_{max} and T_{max} were negatively correlated ($r = -0.5728$; $P = 0.0034$), with early absorbers showing the highest C_{max} values over the T_{max} range of 0.5 to 2.0 h. V (in liters per kilogram) was smallest for the oldest ($r = -0.4707$; $P = 0.0203$) and heaviest ($r = 0.6026$; $P = 0.0018$) subjects. K and $t_{1/2}$ were not correlated strongly with CL_{CR} ($r = \pm 0.0287$ and $P = 0.8941$ for K and $t_{1/2}$). PZA CL did correlate with CL_{CR} ($r = 0.4322$; $P = 0.0349$) and showed a trend toward smaller CL values with advancing age ($r = -0.3669$; $P = 0.0778$). After testing several potential multivariate models, we found a statistically significant relationship between CL (Y variable) and age and CL_{CR} (multiple X variables; analysis of variance; $P = 0.0437$). However, neither X variable alone showed a statistically significant relationship with CL within the context of this model. Height and weight detracted from the fit of the model and were deleted. There also was a correlation between both C_{max} and $AUC_{0-\infty}$ and CL_{CR}, which was expected given their correlations with CL. The pharmacokinetic parameters for the 4 smokers were not statistically different from those for the 20 nonsmokers.

DISCUSSION

Determinations of values of F for INH, RIF, and PZA from the tablet form versus those from an intravenous dosage form were not performed. The programs fit all models to the data assuming that F is equal to 1.

INH. This study used a 250-mg dose of INH, which is lower than the standard daily dose of 300 mg used for adults. This was done to facilitate comparison with the three-drug combination product (data not presented). The estimates for k_a covered a broad range, particularly by the NPEM method. Part of this pattern is likely due to the sampling scheme, which used only four blood draws from 0.5 to 2.0 h and two blood draws from 0.5 to 1.0 h. Better estimates of k_a might have been obtained had additional samples been collected during the first 1 to 2 h after administration of the doses. Because INH does not accumulate appreciably with multiple daily doses, samples

TABLE 5. Absorption characteristics of RIF following administration of a 600-mg dose calculated by noncompartmental methods

C_{max} (μg/ml)				T_{max} (h)				$AUC_{0-\infty}$ (μg · h/ml)			
Mean ± SD	Median	Range	% CV	Mean ± SD	Median	Range	% CV	Mean ± SD	Median	Range	% CV
13.61 ± 3.96	11.80	9.65–24.99	29.1	1.62 ± 0.49[a]	1.50	1.00–3.00	30.2	79.79 ± 27.35	70.62	47.40–142.73	34.3

[a] Interpolated.

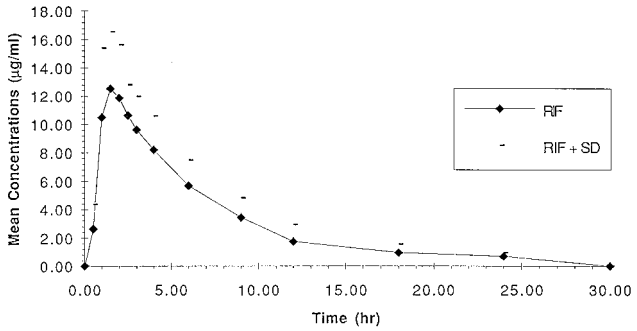

FIG. 3. Mean plasma RIF concentrations across the 24 subjects following administration of a 600 mg-dose of RIF.

obtained as early as the first day of therapy will reflect steady-state values.

The C_{max} and $AUC_{0-\infty}$ values were statistically significantly higher in the 16 slow acetylators compared to those in the 8 fast acetylators. These results were compared to those of a previous study by one of us (C.A.P.) that included seven fast acetylators and five slow acetylators (18). Those data also showed larger $AUC_{0-\infty}$ values for the slow acetylators, but the differences in C_{max} on the basis of acetylator status were smaller and did not reach statistical significance (18). Therefore, differences in C_{max} based on acetylator status may not be evident in all populations.

Fast acetylators had significantly larger CL and *K* values and significantly lower $t_{1/2}$ values compared to those for slow acetylators, regardless of the method used to calculate the values. Similar results were found in our previous study (18). In contrast, the larger estimates of *V* for fast acetylators in the previous study did not reach statistical significance (18). Because we gave oral doses in this study, the differences in the parameter estimates may have reflected differences in *F*. *F* may well have been lower in fast acetylators due to greater first-pass metabolism. The relatively small *V* estimates suggest that INH may not be widely distributed into tissues.

The INH D-optimal sampling times included a point during the absorption phase and either one or two points in the elimination phase, but they were not the true C_{max}. Samples collected at 1.0 h or perhaps at 1.5 h postdose would be preferred for determining C_{max}.

The frequency histograms of individual parameters revealed a bimodal but not a trimodal distribution for CL, *K*, and $t_{1/2}$ (Fig. 2), as described in some studies (21). $t_{1/2}$s based on concentrations in serum at 2 and 6 h were highly correlated with those from the full NCA method, and acetylator status was identical by either approach. This appears to be a reasonable sampling strategy for determining acetylator status. In this study, 67% of the subjects were slow acetylators, which is more than the 50% often described for Caucasians and Hispanics (15, 18, 21).

Using radiometric techniques to study *M. tuberculosis*, Heifets (8) determined the MIC of INH to be 0.025 to 0.05 μg/ml and the minimal bactericidal concentration (MBC) to be 0.05 μg/ml. Based on that, our data indicate that for fast acetylators the median C_{max} of INH (after administration of a dose of 250 mg) is 48 times the MBC and concentrations in serum remain above the MBC until ~8 h postdosing. For slow acetylators, the median C_{max} of INH (after administration of a dose of 250 mg) is 73 times the MBC and concentrations in serum remain above the MBC until ~22 h postdosing. Somewhat higher values would be seen with the standard 300-mg doses. Despite

TABLE 6. Values of pharmacokinetic parameters obtained by various methods for all subjects following administration of an RIF dose of 600 mg

Method	k_a (h^{-1})			Absolute $t_{1/2}$ (h)			*V* (liter/kg)			CL (liters/h)			*K* (h^{-1})			$t_{1/2}$ (h)		
	Mean ± SD	Median	Range	Mean ± SD	Median	Range	Mean ± SD	Median	Range	Mean ± SD	Median	Range	Mean ± SD	Median	Range	Mean ± SD	Median	Range
NCA	NC[a]	NC	NC	NC	NC	NC	0.51 ± 0.10	0.49	0.33–0.74	8.30 ± 2.50	8.50	4.20–12.66	0.21 ± 0.05	0.25	0.12–0.31	3.41 ± 0.86	3.33	2.27–5.55
IT2B, no lag	0.72 ± 0.50	0.58	0.18–1.85	1.49 ± 0.99	1.19	0.38–3.80	0.51 ± 0.09	0.52	0.34–0.63	9.52 ± 2.85	9.26	4.84–14.29	0.25 ± 0.02	0.23	0.13–0.35	3.03 ± 0.87	2.98	1.98–5.28
IT2B, lag	1.94 ± 1.03	1.68	0.77–3.26	0.45 ± 0.22	0.41	0.21–0.90	0.52 ± 0.05	0.53	0.43–0.60	8.46 ± 2.32	8.86	4.84–11.96	0.21 ± 0.04	0.23	0.14–0.26	3.38 ± 0.60	3.07	2.70–4.85
NPEM, no lag	0.79 ± 0.72	0.49	0.18–2.87[b]	0.87[c]	1.41	0.24–3.88	0.50 ± 0.12	0.52	0.10–0.69[b]	9.54 ± 2.90	9.17	4.91–14.57[b]	0.27 ± 0.12	0.23	0.13–0.67[b]	2.56[c]	2.95	1.04–5.50
NPEM, lag	2.57 ± 1.75	1.83	0.77–5.94	0.27[c]	0.38	0.12–0.90	0.54 ± 0.07	0.51	0.42–0.69	8.59 ± 2.36	8.67	4.86–12.24	0.21 ± 0.04	0.20	0.11–0.27	3.34[c]	3.40	0.26–6.39

[a] NC, not calculated.
[b] Approximate range, from 2.5 to 97.5%, as calculated by NPEM.
[c] Calculated as $\ln(2)/k_a$ or $\ln(2)/K$ from the population means and not across the individual point estimates. Therefore, no SD is included.

TABLE 7. NPEM analyses with and without lag phase for smooth and low absorbers of RIF[a]

Group	No. of subjects	Log likelihood	k_a (h^{-1})	Absorption (h)	V (liter/kg)	CL (liters/h)	K (h^{-1})	$t_{1/2}$ (h)
Smooth, no lag	14	−245.09	1.27	0.55	0.52	8.55	0.21	3.27
Smooth, with lag	14	−225.63	3.90	0.18	0.61	8.71	0.21	3.37
Low, no lag	10	−263.98	0.35	2.00	0.27	6.58	0.31	2.21
Low, with lag	10	−210.55	1.25	0.56	0.55	9.12	0.22	3.19
All, no lag	24	−1,220.56	0.49	1.41	0.52	9.17	0.23	2.95
Smooth, no lag, and low with lag	24	−458.64	1.25	0.55	0.54	8.73	0.21	3.23
All lag	24	−445.50	1.83	0.38	0.51	8.67	0.20	3.40

[a] Values are medians for the subject population.

these differences, both acetylator types have roughly equivalent responses to treatment in clinical trials except when the dosing interval is extended to once weekly (21). In that seldom used regimen, slow acetylators had better responses (21).

RIF. The NPEM models revealed two groups of RIF absorbers: smooth absorbers and those who have low RIF concentrations followed by rapid absorption (low absorbers). Part of this pattern is likely due to the sampling scheme, which used only four blood draws from 0.5 to 2.0 h. These groups may not have been distinguishable had additional samples been collected during the first 2 h after administration of the doses. Alternatively, they may have been more distinguishable. The ability to discover such unsuspected subpopulations is a unique feature of the nonparametric modeling methods such as NPEM, because they make no preconceived assumptions concerning the shape of the parameter joint probability density. In contrast, parametric methods such as the IT2B method obtain means, SDs, and covariances and assume that the shape of the distribution is Gaussian.

The negative correlation between both height and weight and the C_{max} values suggests that the dosing of RIF on a milligram-per-kilogram basis would be appropriate for all patients. Currently, RIF is given as 450 mg to adults weighing <50 kg and 600 mg to those weighing ≥50 kg (1). In order to achieve similar concentration-versus-time profiles, very large patients (>75 kg) should probably receive doses of 750 mg or more. Current recommendations arbitrarily limit doses to a daily maximum of 600 mg (1). Of note, the influenza-like syndrome seen with RIF has only been associated with doses of >900 mg given two to three times each week and has not been reported with daily doses (1, 17). Limiting doses to 600 mg may lead to suboptimal plasma RIF concentration profiles in large patients.

The clearance of RIF is predominantly through nonrenal mechanisms, with only 10% of the drug reported to be cleared unchanged in the urine over 24 h (10, 15). Consistent with these facts, we found only a weak correlation between CL and CL_{CR}. RIF is converted to 25-desacetylrifampin and other, less abundant metabolites, which are subsequently cleared through nonrenal and, to a lesser extent, renal mechanisms (9, 10, 13, 15). 25-Desacetylrifampin retains some activity against several organisms and is present at concentrations in serum that are roughly 10% of those of RIF (9, 10, 13, 15).

The RIF D-optimal sampling times included a point during the absorptive phase and either one or two points in the elimination phase, but they were not the true C_{max}. The three-sample strategy (no lag) included a 0.6-h time point, and both the two- and three-sample strategies for the lag phase models included a time point of ≤0.7 h, even though 13 of 24 subjects did not have quantifiable RIF concentrations in their blood until 1.0 h. Adding back an average lag time of 0.52 h or a median lag time of 0.75 h produces a sampling time of >1.0 h when the sera of all subjects had measurable concentrations. Samples collected at 1.5 h or perhaps 2.0 h postdose would be preferred for determining C_{max}.

Using radiometric techniques to study *M. tuberculosis*, Heifets (8) determined the MIC of RIF to be 0.06 to 0.25 μg/ml and the MBC to range from 0.06 to 0.5 μg/ml. Based on that, our data indicate that the median RIF C_{max} is ~24 times the MBC, and concentrations in serum remain above the MBC until ~17 h postdosing at the outset of treatment. Because the $t_{1/2}$ of RIF decreases to ~2 h over the first 6 to 14 days of treatment due to more rapid clearance, the time that plasma RIF concentrations exceed the MBC will decline toward 11 h postdosing (10, 15).

PZA. PZA was rapidly absorbed, with most T_{max} values being near 1 h. Variability across the 24 subjects was minimal, especially for the C_{max} and $AUC_{0-\infty}$ values. While the steady state was achieved after 4 days of simulated dosing, the simulated concentrations in serum on day 2 approached the steady-state values. Therefore, sampling can be performed as early as day 2 of treatment and will reflect steady-state concentrations. The negative correlation between both height and weight and the C_{max} values suggests that the current clinical practice of dosing PZA on a milligram-per-kilogram basis is appropriate.

The long $t_{1/2}$ of PZA (approximately 10 h) renders it suitable for once-daily dosing, particularly since it is used against the slowly growing organism *M. tuberculosis*, which has doubling times of ≥24 h. The clearance of PZA is predominantly through nonrenal mechanisms, with only 4% of the drug reported to be cleared unchanged in the urine over 24 h (15, 23). PZA is largely converted to pyrazinoic acid and 5-hydroxy-

TABLE 8. Absorption characteristics for PZA following administration of a 1,500-mg dose calculated by noncompartmental methods

C_{max} (μg/ml)				T_{max} (h)				$AUC_{0-\infty}$ (μg · h/ml)			
Mean ± SD	Median	Range	% CV	Mean ± SD	Median	Range	% CV	Mean ± SD	Median	Range	% CV
29.21 ± 4.35	28.81	21.70–42.64	14.9	1.17 ± 0.41[a]	1.00	0.50–2.00	35.0	415.46 ± 67.26	396.64	303.55–541.36	16.7

[a] Interpolated.

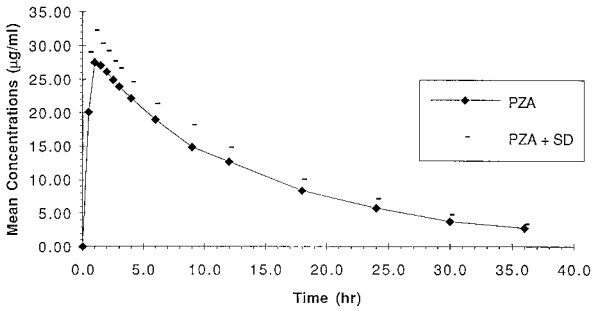

FIG. 4. Mean plasma PZA concentrations across the 24 subjects following administration of a 1,500-mg dose of PZA.

pyrazinoic acid, which are subsequently cleared through renal and nonrenal mechanisms (15, 23). The weak correlation found between CL and CL_{CR} is consistent with these facts. It should be noted that CL_{CR} ranged from 72 to 130 ml/min in these healthy volunteers, and we could not test the relationship between CL and CL_{CR} in the presence of renal dysfunction in this population.

The D-optimal sampling times for PZA included a point during the absorptive phase and either one or two points in the elimination phase, but they were not the true C_{max}. Samples collected at 1.0 h or as late as 2.0 h postdose would be preferred for determining C_{max}.

PZA displays a pH-dependent MIC against *M. tuberculosis* (8). Using radiometric techniques, Heifets (8) determined the MIC of PZA at pH 5.5 to be 6.2 to 50 μg/ml for *M. tuberculosis*. However, PZA is believed to be most active at lower pH values, and the in vitro cultivation of *M. tuberculosis* is not possible at lower pH values (8). Furthermore, the mechanism of action of PZA is poorly understood, and the relative importance of PZA versus that of its active metabolite, pyrazinoic acid, remains to be defined. Therefore, we have not calculated C_{max}:MIC or time above MIC for PZA.

All three drugs. *M. tuberculosis* grows slowly in vitro and appears to display various growth rates in vivo, ranging from continuous growth to complete dormancy (8). Given these different populations of organisms, it may prove to be difficult to correlate drug efficacy with derived parameters such as C_{max}:MIC, AUC above MIC, or time of the concentration above the MIC (8, 17, 19). The activities of drugs against the extracellular, rapidly growing population has been described in terms of the early bactericidal effect (8). This population behaves most like typical bacteria. Relating the derived parameters to drug efficacy against other populations (intracellular, semidormant, or dormant organisms) is more problematic. The activities of drugs against these populations have been described as sterilizing activity. This process is slow, requiring treatment regimens of 6 months or longer. Additional research is needed to explore how the derived parameters can be used to optimize antituberculosis drug therapy.

Recent reports have raised concerns about altered pharmacokinetics of antimycobacterial drugs in various patient subpopulations, including patients with AIDS (3, 14, 16, 19, 20, 22). In some cases, drug malabsorption has been associated with clinical failures and the selection of drug-resistant *M. tuberculosis*. We are currently studying INH, RIF, PZA, and the other antimycobacterial drugs with these patient populations to see how the pharmacokinetic behaviors of these drugs may differ from those seen in healthy volunteers.

Conclusions. The concentrations in plasma and the pharmacokinetic parameters found in this study were consistent with

TABLE 9. Estimates of values of pharmacokinetic parameters for PZA following administration of a PZA dose of 1,500 μg

Method	k_a (h^{-1})			Absolute $t_{1/2}$ (h)			V (liter/kg)			CL (liters/h)			K (h^{-1})			$t_{1/2}$ (h)		
	Mean ± SD	Median	Range	Mean ± SD	Median	Range	Mean ± SD	Median	Range	Mean ± SD	Median	Range	Mean ± SD	Median	Range	Mean ± SD	Median	Range
NCA	NC[a]	NC	NC	NC	NC	NC	0.70 ± 0.08	0.69	0.60–0.93	3.70 ± 0.59	3.78	2.77–4.94	0.07 ± 0.01	0.07	0.05–0.09	10.08 ± 1.29	10.12	8.13–12.94
IT2B	3.25 ± 2.36	2.58	0.65–8.51	0.36 ± 0.29	0.27	0.08–1.06	0.68 ± 0.06	0.69	0.58–0.80	3.74 ± 0.60	3.79	2.78–5.04	0.07 ± 0.01	0.07	0.05–0.10	9.73 ± 1.33	10.06	7.14–12.62
NPEM	4.62 ± 5.22	2.47	0.66–18.70[b]	0.15[c]	0.28	0.04–1.05[b]	0.68 ± 0.06	0.68	0.58–0.79[b]	3.76 ± 0.59	3.80	2.76–4.98[b]	0.07 ± 0.01	0.07	0.05–0.10[b]	9.58[c]	10.00	7.15–13.08[b]

[a] NC, Not calculated.
[b] Approximate range, from 2.5 to 97.5%, as calculated by NPEM.
[c] Calculated as $\ln(2)/k_a$ or $\ln(2)/K$ from the population means and not across the individual point estimates. Therefore, no SD is included.

those described previously (6, 10, 15, 18, 23). The NCA, IT2B, and NPEM methods all produced results that were in agreement, suggesting that any of these methods would be appropriate for describing data for INH, RIF, or PZA in healthy volunteers. Clinically, these models can serve as benchmarks for comparison with models for other populations, like patients with tuberculosis or tuberculosis and AIDS. Samples drawn as early as day 1 of daily INH therapy will show concentrations in serum that mirror steady-state values. Because RIF clearance increases over the first week of treatment, blood samples should be obtained after 7 days of treatment. Samples drawn as early as day 2 of daily PZA therapy will produce concentrations in serum that approach steady-state values.

ACKNOWLEDGMENTS

This study was supported in part by NIH grants RO1 AI37845 and LM 05401.

REFERENCES

1. **American Thoracic Society/Centers for Disease Control.** 1994. Treatment of tuberculosis and tuberculosis infection in adults and children. Am. J. Respir. Crit. Care Med. **149:**1359–1374.
2. **Anonymous.** 1983. 1983 Metropolitan height and weight tables. Stat. Bull. Metrop. Life Foundation **64:**3–9.
3. **Berning, S. E., G. A. Huitt, M. D. Iseman, and C. A. Peloquin.** 1992. Malabsorption of antituberculosis medications by an AIDS patient N. Engl. J. Med. **327:**1817–1818. (Letter.)
4. **Cockroft, D. W., and M. H. Gault.** 1976. Prediction of creatinine clearance from serum creatinine. Nephron **10:**31–41.
5. **D'Argenio, D., and A. Schumitzky.** 1992. ADAPT II user's guide, biomedical simulations resource. University of Southern California, Los Angeles.
6. **Ellard, G. A.** 1969. Absorption, metabolism and excretion of pyrazinamide in man. Tubercle **50:**144–158.
7. **Gibaldi, M., and D. Perrier.** 1982. Pharmacokinetics, 2nd ed. Marcel Dekker, Inc., New York, N.Y.
8. **Heifets, L. B.** 1991. Antituberculosis drugs: anti-microbial activity *in vitro*, p. 13–58. *In* L. B. Heifets (ed.), Drug susceptibility in the chemotherapy of mycobacterial infections. CRC Press, Inc., Boca Raton, Fla.
9. **Houin, G., A. Beucler, S. Richelet, R. Brioude, C. Lafaix, and J. P. Tillement.** 1983. Pharmacokinetics of rifampicin and desacetylrifampicin in tuberculosis patients after different rates of infusion. Ther. Drug Monit. **5:**67–72.
10. **Iwainsky, H.** 1988. Mode of action, biotransformation and pharmacokinetics of antituberculosis drugs in animals and man, p. 399–553. *In* K. Bartmann (ed.), Antituberculosis drugs. Springer-Verlag, Berlin, Germany.
11. **Jelliffe, R. W.** 1989. Explicit determination of laboratory assay error patterns: a useful aid in therapeutic drug monitoring, p. 1–6. ASCP Clinical Pharmacology Check Sample 10, No. DM 89-4 (DM 56). American Society of Clinical Pathologists, Chicago, Ill.
12. **Jelliffe, R. W., A. Schumitzky, and M. Van Guilder.** 1996. User manual for version 10.6 USC*PACK collection of PC programs. Laboratory of Applied Pharmacokinetics, University of Southern California, Los Angeles.
13. **Mouton, R. P., H. Mattie, K. Swart, J. Kreukniet, and J. de Wael.** 1979. Blood levels of rifampicin, desacetylrifampicin, and isoniazid during combined therapy. J. Antimicrob. Chemother. **5:**447–454.
14. **Patel, K. B., R. Belmonte, and H. M. Crowe.** 1995. Drug malabsorption and resistant tuberculosis in HIV-infected patients. N. Engl. J. Med. **332:**336–337. (Letter.)
15. **Peloquin, C. A.** 1991. Antituberculosis drugs: pharmacokinetics, p. 59–88. *In* L. B. Heifets (ed.), Drug susceptibility in the chemotherapy of mycobacterial infections. CRC Press, Inc., Boca Raton, Fla.
16. **Peloquin, C. A., A. A. MacPhee, and S. E. Berning.** 1993. Malabsorption of antimycobacterial medications. N. Engl. J. Med. **329:**1122–1123. (Letter.)
17. **Peloquin, C. A., and S. E. Berning.** 1994. Infection due to *Mycobacterium tuberculosis*. Ann. Pharmacother. **28:**72–84.
18. **Peloquin, C. A., G. T. James, L. D. Craig, M. Kim, E. A. McCarthy, D. N. Iklé, and M. D. Iseman.** 1994. Pharmacokinetic evaluation of aconiazide, a potentially less toxic isoniazid pro-drug. Pharmacotherapy **14:**415–423.
19. **Peloquin, C. A.** 1996. Therapeutic drug monitoring of the antimycobacterial drugs. Clin. Lab. Med. **16:**717–729.
20. **Peloquin, C. A., A. T. Nitta, W. J. Burman, K. F. Brudney, J. R. Miranda-Massari, M. E. McGuinness, S. E. Berning, and G. T. Gerena.** 1996. Low anti-tuberculosis drug concentrations in patients with AIDS. Ann. Pharmacother. **30:**919–925.

20a. **Peloquin, C. A., G. S. Jaresko, C. L. Yong, A. C. F. Keung, and R. W. Jelliffe.** 1996. Population pharmacokinetic models of isoniazid (INH), rifampin (RIF), & pyrizinamide (PZA), abstr. A89, p. 17. *In* Program and abstracts of the 36th Interscience Conference on Antimicrobial Agents and Chemotherapy. American Society for Microbiology, Washington, D.C.

21. **Relling, M. V., and W. E. Evans.** 1992. Genetic polymorphisms of drug metabolism, p. 7-1–7-32. *In* W. E. Evans, J. J. Schentag, and W. J. Jusko (ed.), Applied pharmacokinetics: principles of therapeutic drug monitoring. Applied Therapeutics, Inc., Vancouver, Wash.
22. **Sahai, J., K. Gallicano, L. Swick, S. Tailor, G. Garber, I. Seguin, L. Oliveras, S. Walker, A. Rachlis, and D. W. Cameron.** 1997. Reduced plasma concentrations of antituberculosis drugs in patients with HIV infection. Ann. Intern. Med. **127:**289–293.
23. **Stottmeier, K. D., R. E. Beam, and G. P. Kubica.** 1968. The absorption and excretion of pyrazinamide. I. Preliminary study in laboratory animals and in man. Am. Rev. Respir. Dis. **98:**70–74.